October 2007

A highly compact third-order silicon microring add-drop filter with a very large free spectral range, a flat passband and a low delay dispersion

Shijun Xiao
Purdue University, sxiao@purdue.edu

Maroof H. Khan
Birck Nanotechnology Center, Purdue University, mhkhan@purdue.edu

Hao Shen
Purdue University - Main Campus, shen17@purdue.edu

Minghao Qi
Birck Nanotechnology Center, Purdue University, mqi@purdue.edu

A highly compact third-order silicon microring add-drop filter with a very large free spectral range, a flat passband and a low delay dispersion

Shijun Xiao, Maroof H. Khan, Hao Shen and Minghao Qi

Birck Nanotechnology Center, Purdue University, West Lafayette, IN 47907, USA
sxiao@purdue.edu, mqi@purdue.edu

Abstract – We demonstrate highly compact third-order silicon microring add-drop filters. The microring resonator has a small radius of 2.5 μm and a very large free spectral range of 32 nm at 1.55 μm. Experimental results show a low add-drop crosstalk of around -20 dB. Box-like channel dropping response is demonstrated, and it has a passband of ~ 1 nm (125 GHz), fast rolling-off (slope ~ 0.2 dB/GHz), high out-of-band signal rejection of around 40 dB and a low drop loss. Simulation agrees well with experiments in power transmission, and the group delay is also simulated and the variation is less than 1 ps within the passband. The propagation loss in microring resonators is optimized.

OCIS codes: 250.5300 (photonic integrated circuits); 130.3120 (integrated optical devices); 230.5750 (resonators); 220.4000 (microstructure fabrication)

References and links

1. B. E. Little, J. S. Foresi, G. Steinmeyer, E. R. Thoen, S. T. Chu, H. A. Haus, E. P. Ippen, L. C. Kimerling, and W. Greene, "Ultra-compact Si-SiO2 microring resonator optical channel dropping filters," IEEE Photon. Technol. Lett. **10**, 549-551 (1998).
2. A. Vörckel, M. Mönster, W. Henschel, P. H. Bolivar, and H. Kurz, "Asymmetrically coupled silicon-on-insulator microring resonators for compact add-drop mutiplexers," IEEE Photon. Technol. Lett. **15**, 921-923 (2003).
3. P. Dumon, W. Bogaerts, V. Wiaux, J. Wouters, S. Beckx, J. V. Campenhout, D. Taillaert, B. Luyssaert, P. Bienstman, D. V. Thourhout, and R. Baets, "Low loss SOI photonic wires and ring resonators fabricated with deep UV lithography," IEEE Photon. Technol. Lett. **16**, 1328-1330 (2004).
4. T. Barwicz, M. A. Popovíc, P. Rakich, M. Watts, H. Haus, E. Ippen, and H. Smith, "Microring-resonator based add-drop filters in SiN: fabrication and analysis," Opt. Express **12**, 1437-1442 (2004).
5. T. Barwicz, M.A. Popović, M. R. Watts, P. T. Rakich, E. P. Ippen and H. I. Smith, "Fabrication of Add-Drop Filters Based on Frequency-Matched Microring Resonators," IEEE J. Lightwave Technol. **24**, 2207-2218 (2006).
6. M. A. Popovíc, T. Barwicz, M. R. Watts, P. T. Rakich, L. Socci, E. P. Ippen, F. X. Kärtner, and H. I. Smith, "Multistage high-order microring-resonator add-drop filters," Opt. Lett. **31**, 2571-2573 (2006).
7. M. A. Popovíc, T. Barwicz, F. Gan, M. S. Dahlem, C. W. Holzwarth, P. T. Rakich, H. I. Smith, E. P. Ippen and F. X. Kärtner, "Transparent wavelength switching of resonators," in Conference on Lasers and Electro-Optics 2007 Technical Digest (Optical Society of America, Washington, DC, 2007), paper CPDA2.
8. F. Xia, M. Rooks, L. Sekaric, and Y. A. Vlasov, "Ultra-compact silicon WDM optical filters with flat-top response for on-chip optical interconnects," in Conference on Lasers and Electro-Optics 2007 Technical Digest (Optical Society of America, Washington, DC, 2007), paper CTuG3.
9. M. A. Popovíc, C. Manolatou, and M. R. Watts, "Coupling-induced resonance frequency shifts in coupled dielectric multi-cavity filters," Opt. Express **14**, 1208-1222 (2006).
10. S. Xiao, M. H. Khan, H. Shen, and M. Qi, "Multiple-channel silicon micro-resonator based filters for WDM applications," Opt. Express **15**, 7489-7498 (2007).
11. B. E. Little, S. T. Chu, H. A. Haus, J. Foresi, and J. P. Laine, "Microring resonator channel dropping filters," IEEE J. Lightwave Technol. **15**, 998-1005 (1997).
12. S. Xiao, M. H. Khan, H. Shen, and M. Qi, "Modeling and measurement of losses in silicon-on-insulator resonators and bends," Opt. Express **15**, 10553-10561 (2007).

#86165 - $15.00 USD Received 9 Aug 2007; revised 5 Oct 2007; accepted 9 Oct 2007; published 24 Oct 2007

13. S. Xiao, M. H. Khan, H. Shen, and M. Qi, "Silicon-on-insulator microring add-drop filters with free spectral ranges over 30 nm," submitted, IEEE J. Lightwave Technol.
14. S. Xiao, M. H. Khan, H. Shen, and M. Qi, "Compact silicon microring resonators with ultra-low propagation loss in the C band," accepted with revision, Opt. Express **15** (2007).

1. Introduction

The high-index-contrast in silicon-on-insulator (SOI) waveguides allows small bend radii with low propagation losses, leading to compact microring resonators and high-density integration of micro-photonic devices. SOI microring add-drop filters [1-3] are promising for WDM signal processing in a silicon chip. However, it is challenging to achieve simultaneously large free spectral range (*FSR*) to cover the entire C telecom window, box-like response with maximally flat passband, fast rolling-off and high out-of-band signal rejection, and low add-drop crosstalk in SOI microring optical add-drop filters. Recently, microring add-drop filters were reported both in silicon nitride (SiN) [4-6] and in silicon [7-8], and reported micoring resonators have a *FSR* of 20 nm (microring's radius ~ 8 μm) [4-6], 16 nm (microring's radius ~ 5 μm) [7] and around 10 nm with racetrack resonators [8]. The authors mainly focused on wavelength switching applications in [7] with few details provided on microring add-drop filter. Compared to racetrack resonators with the same *FSR*, ring resonators offer the smallest footprint and the lowest propagation loss. In this paper, we demonstrate a very large *FSR* of 32 nm at 1.55 μm in third-order silicon microring add-drop filters with a ring radius of 2.5 μm. Nevertheless, the propagation loss in small microring resonators can be large due to the sharp bending, and this nontrivial propagation loss has increased significantly the complexity in designing microring add-drop filters. Compared to the majority of previously reported microring add-drop filters, our demonstrated microring add-drop filters have the smallest footprint for integration and the largest *FSR* covering almost the whole spectral range of C band. Low add-drop crosstalk ~ -20 dB, low drop loss and box-like response with very flat passband and high out-of-band signal rejection of ~ 40 dB are achieved. Our devices were fabricated with electron-beam lithography (EBL), and coupling induced resonance wavelength mismatch [9] is compensated by dose control in EBL [5]. With our recently reported multiple-channel scheme [10], the demonstrated third-order filter can be configured in a multiple-channel structure that is truly compatible with WDM systems.

2. Device fabrication

Our devices were fabricated in a silicon-on-insulator (SOI) wafer with a top silicon layer thickness of 250 nm and a buried oxide thickness of 3 μm. The device patterns were exposed in a 150 nm-thick negative resist (hydrogen silsesquioxane: HSQ) with a Vistec 100 kV EBL system installed in the Birck Nanotechnology Center at Purdue University. The main beam deflection field size is 0.5mm×0.5mm, and the beam deflection step is 2 nm. The etching of silicon was done in an inductively-coupled-plasma (ICP) reactive-ion-etcher with Cl_2.

3. Filter design and experiments

Figure 1 shows a schematic symmetrically coupled third-order microring add-drop filter. All three microring resonators are identical in geometry and have center resonance wavelengths represented by λ_1, λ_2 and λ_3, respectively. Ideally, we should have $\lambda_1=\lambda_3$ due to symmetry. g is the gap between bus waveguides and microring resonators, and g_m is the gap between microring resonators. κ^2 is the power coupling coefficient between bus waveguides and microring resonators, and κ_m^2 is the mutual power coupling coefficient between microring resonators. The propagation power loss coefficient is κ_p^2 per round-trip in each microring resonator. The *FSR* can be expressed by $FSR=\lambda^2/(2\pi\times Rn_g)$, where n_g is the group index. For maximally flat drop passband, if κ_p^2 is negligible [11] or $\kappa^2 \gg \kappa_p^2$ in our case, $\kappa_m^2=\kappa^4/8$ [11] should hold. This indicates $\kappa_m^2<\kappa^2$, and consequently $g_m>g$. Due to coupling induced

#86165 - $15.00 USD Received 9 Aug 2007; revised 5 Oct 2007; accepted 9 Oct 2007; published 24 Oct 2007

resonance wavelength shift [9], $\lambda_1=\lambda_3<\lambda_2$. To match the middle resonator's center resonance wavelength with that of the other two resonators, one option is to reduce W_{ring} slightly, and this can be achieved by exposing the center ring with slightly lower dose in EBL. Although the coupling induced resonance wavelength shift can be perfectly compensated in theory, all three resonators do not have exactly the same center resonance wavelength as there are always inevitable fabrication imperfections. The phase matching in each resonator is very sensitive to even a very small amount of change in dimensions or index distribution for high-index-contrast waveguides. In EBL, there are also digitization errors and beam deflection errors that can cause very small dimension errors of only a few nanometers in microring resonators. Thus, it is conservative to assume $\lambda_1 \neq \lambda_2 \neq \lambda_3$.

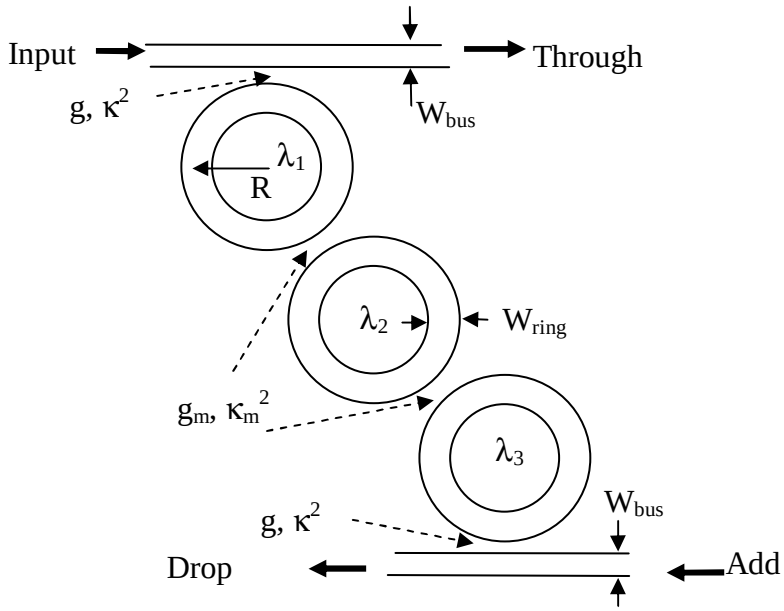

Fig.1. Schematic drawing of a symmetrically coupled third-order microring resonator.

With the developed coupled-mode-theory (CMT) in time [11], it can be shown that the add-drop response in wavelength domain parameters [12] of a third-order microring filter can be obtained by solving the following matrix equation:

$$\begin{bmatrix} -j\frac{\lambda-\lambda_1}{FSR}+\frac{\left(\kappa^2+\kappa_p{}^2\right)}{4\pi} & j\frac{\kappa_m}{2\pi} & 0 \\ j\frac{\kappa_m}{2\pi} & -j\frac{\lambda-\lambda_2}{FSR}+\frac{\kappa_p{}^2}{4\pi} & j\frac{\kappa_m}{2\pi} \\ 0 & j\frac{\kappa_m}{2\pi} & -j\frac{\lambda-\lambda_3}{FSR}+\frac{\left(\kappa^2+\kappa_p{}^2\right)}{4\pi} \end{bmatrix} \times \begin{bmatrix} s_1 \\ s_2 \\ s_3 \end{bmatrix} = \begin{bmatrix} \frac{\kappa^2}{2\pi} \\ 0 \\ 0 \end{bmatrix} \qquad (1)$$

where s_1, s_2 and s_3 represents normalized complex wave field in a lumped coupled resonator system. Complex amplitude transmission is then expressed by $t_{through}=1-s_1$ and $t_{drop}= -s_3$ for the through-port and the drop-port, respectively. The corresponding power transmissions are $|t_{through}|^2$ and $|t_{drop}|^2$, respectively.

It is known that the propagation loss decreases as the waveguide width increases in silicon waveguides, as the guided light is more confined in the silicon core and scatters less at the rough surfaces of the waveguides. The microring waveguide is approximately of single mode

#86165 - $15.00 USD Received 9 Aug 2007; revised 5 Oct 2007; accepted 9 Oct 2007; published 24 Oct 2007

(the lowest TE) at ~ 1.55 μm for waveguide's width up to 600 nm, and other modes have higher propagation losses in the strongly bended microring waveguides. With a recently reported method [12], propagation losses in fabricated microring resonators with $R=2.5$ μm and different W_{ring} were characterized and listed in the following table:

Tab. 1 The propagation loss and the power loss ratio per round trip in microring resonators

W_{ring} (nm)	450	500	550	600
Loss (dB/mm)	31±3	13±1	7.5±1	4.5±0.5
κ_p^2	0.108±0.01	0.046±0.005	0.027±0.003	0.016±0.002
$Q_{intrinsic}$	3000±300	7000±700	12000±1200	20000±2000

Detailed loss analysis for 2.5 μm-radius microrings were presented in ref. [13]. The propagation loss was reduced down to ~ 2 dB/cm in 10 μm-radius microrings [14], corresponding to intrinsic quality factors up to ~ 400,000. However, the free spectral range was reduced to around 8 nm.

In our fabricated third-order microring add-drop filters, W_{ring} is set to 600 nm for low propagation loss, which is very important to achieve low add-drop crosstalk as well as low drop loss [12]. Waveguide power coupling should follow $\kappa^2 \geq \sim 10\times\kappa_p^2$ for an add-drop crosstalk ≤ -20 dB and a low drop loss. However, it must be noted that the add-drop filter performance can degrade due to mismatched resonance wavelengths between rings. Figure 2 shows scanning-electron micrographs of one fabricated third-order microring filter. We have W_{ring}=600±10 nm and W_{bus}=500±10 nm. Coupling gaps $\{g, g_m, g_m, g\}$ are calibrated to be {100±10, 350±10, 350±10, 100±10} nm. The coupling gaps were designed to satisfy both $\kappa^2 \geq \sim 10\times\kappa_p^2$ and $\kappa_m^2=\kappa^4/8$. In our case, the middle microring pattern was exposed with a 3.5% lower dose than the other two microrings in EBL in order to compensate the coupling induced resonance wavelength mismatch.

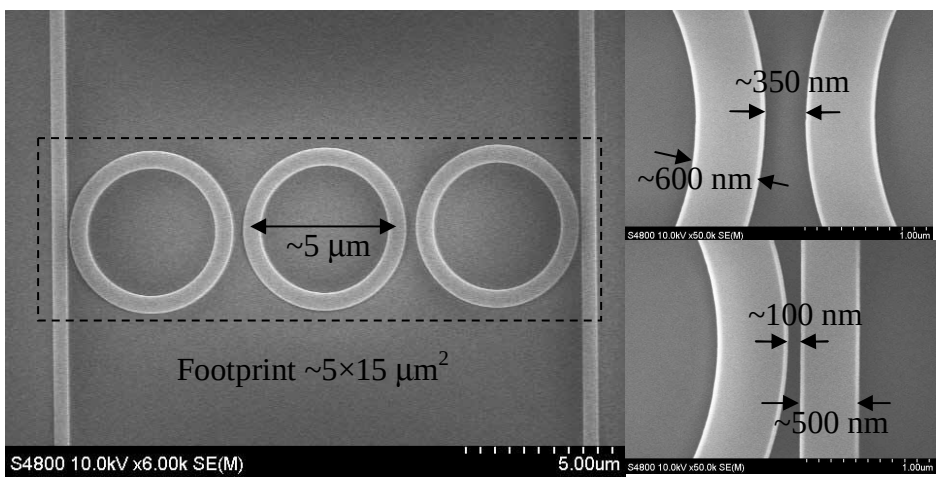

Fig. 2. Scanning-electron micrographs of one fabricated third-order microring add-drop filter. The right ones are zoom-in views of waveguide coupling region (50K magnification).

Figure 3 shows measured data of power transmission for both the through-port (red) and the drop-port (blue). The drop-port transmission is normalized to the through-port transmission by setting the through-port transmission to 0 dB (100%) at non-resonating wavelengths. A very large free spectral range of ~ 32 nm is achieved, which can cover almost

#86165 - $15.00 USD Received 9 Aug 2007; revised 5 Oct 2007; accepted 9 Oct 2007; published 24 Oct 2007

the entire C band (~ 1535-1565nm). Box-like responses are achieved with out-of-band signal rejection of 40 dB.

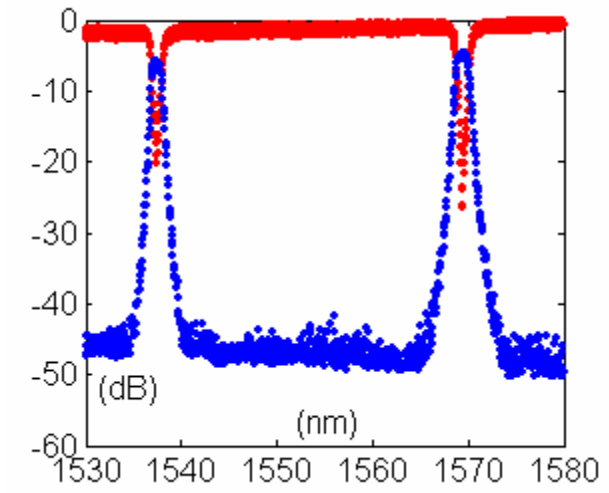

Fig. 3. Experimental responses of the fabricated third-order microring add-drop filter.

Figures 4(a)-4(b) provide detailed analysis of each add-drop filtering response for two resonance bands shown in Fig. 3. Simulated responses are plotted to compare with experimental responses. In Fig. 4(a), the black lines are simulated responses for κ^2=0.19, k_m^2=0.006, k_p^2=0.016, *FSR*=32 nm and $\lambda_1=\lambda_2=\lambda_3$, and the green lines are simulated responses for κ^2=0.19, k_m^2=0.006, k_p^2=0.016, *FSR*=32 nm as well as resonance wavelength mismatch of λ_1-λ_2= -0.18 nm and λ_1-λ_3=-0.25 nm. The method published in [12] was used to extract the waveguide-to-ring power coupling coefficient κ^2, and an approximate exponential model [11] was used to design the ring's mutual power coupling coefficient κ_m^2. The channel dropping response has a very flat passband, which is not sensitive to small resonance wavelength mismatch. The channel dropping -1dB bandwidth, -3dB bandwidth, -20dB bandwidth and -30 dB bandwidth are 0.85±0.05, 1.15±0.05, 2.45±0.05 and 3.20±0.05 nm, respectively. The roll-off slope is around 25dB/nm or 0.2 dB/GHz. Compared to the roll-off slope reported in [5-6], our achieved number is approximately 50% smaller, and this is due to the larger propagation loss in microrings with such a small radius of 2.5 μm. In principle, a channel spacing of 200GHz is feasible with adjacent channel cross-talk of -30 dB. The theoretical channel dropping loss is 1.5 dB, and the experimental drop-port response is shifted 3.5 dB vertically in order to match the theoretical drop-port response. This discrepancy of loss is likely due to different fiber-to-waveguide couplings and propagation losses in silicon waveguides of ~ 5 mm long between the through-port and the drop-port [12]. The through-port response is very sensitive to small resonance wavelength mismatch as it was reported in [5-6]. Due to small residual resonance mismatch, the add-drop crosstalk increases to around -20dB from the simulated one of -30dB, and the through-port response changes to an asymmetric lineshape from the symmetric lineshape. The add-drop crosstalk is limited by small uncompensated resonance wavelength mismatch, caused by inevitable fabrication imperfections, e.g., electron-beam deflection errors over the field. As it was discussed in [5], a very tight control in fabrication on waveguide dimensions should be applied to reduce the resonance wavelength mismatch. In Fig. 4(b), the black lines are simulated responses for κ^2=0.28, k_m^2=0.009, k_p^2=0.035, *FSR*=32 nm and $\lambda_1=\lambda_2=\lambda_3$. The channel dropping -1dB bandwidth, -3dB bandwidth and -20dB bandwidth are 0.90±0.05, 1.30±0.05 and 3.20±0.05 nm, respectively. The roll-off slope is about 17 dB/nm or 0.14 dB/GHz. The theoretical

#86165 - $15.00 USD Received 9 Aug 2007; revised 5 Oct 2007; accepted 9 Oct 2007; published 24 Oct 2007

channel dropping loss is 2.3 dB, and the experimental drop-port response is shifted 2 dB vertically up in order to match the theoretical drop-port response. Similar to Fig. 4(a), there are small residual resonance mismatch that causes an asymmetric lineshape of the through-port response as well as an increased add-drop crosstalk within the passband.

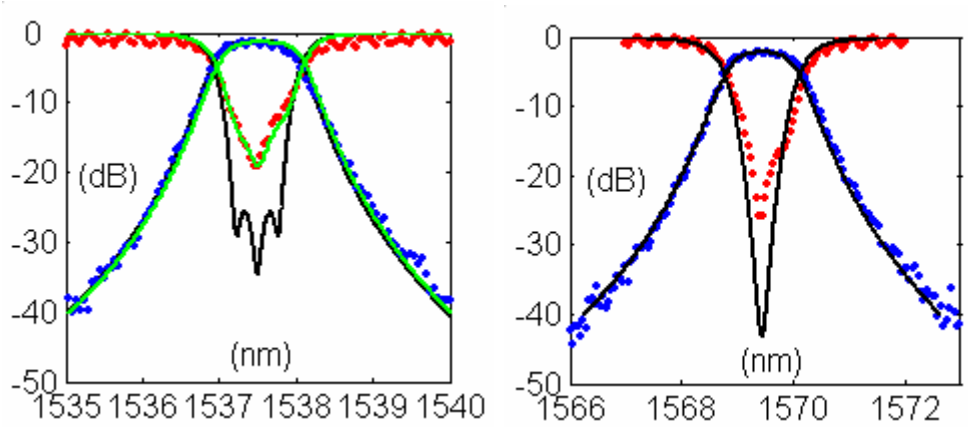

(a) (b)

Fig. 4. Comparison of add-drop responses between simulation and experiments. The drop responses were shifted up vertically by 3.5 dB in (a) and 2 dB in (b) to match the simulated responses where no additional losses were accounted.

Figures 5(a)-5(b) show corresponding simulated group delays for channel dropping responses in Figs. 4(a)-4(b), respectively. Within the flat passband of ~ 1 nm bandwidth, the group delay reaches minimum at the center resonance wavelength, and the relative change is less than 1 ps. For a 125 GHz channel bandwidth, e.g., supporting 40 Gbps high-speed data, this phase dispersion effect is very small. The group delays are obviously different for two center resonance wavelengths, indicating different group velocities at different wavelengths in microring resonators. Additionally, a flat group delay within the passband can be designed for a Gaussian-like power or amplitude response, and it is a simple trade-off between flat group delay and flat power response.

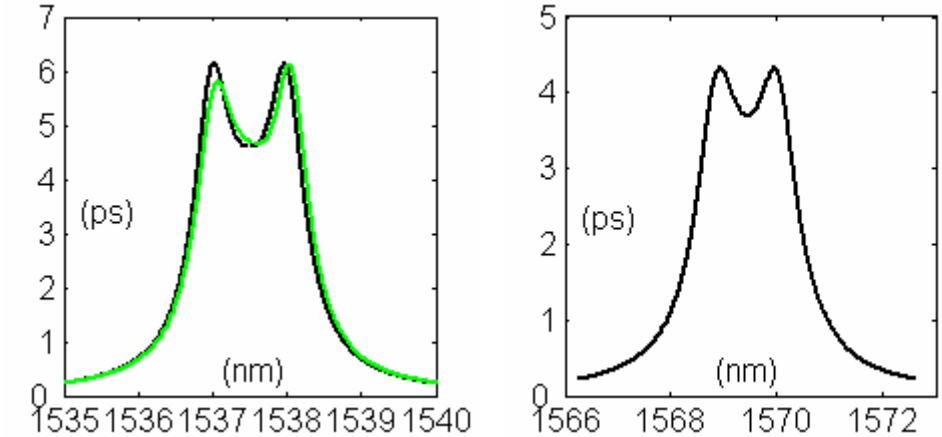

(a) (b)

Fig. 5. Simulated relative group delays in channel dropping passband for two resonance wavelength bands.

#86165 - $15.00 USD Received 9 Aug 2007; revised 5 Oct 2007; accepted 9 Oct 2007; published 24 Oct 2007

4. Conclusion

In summary, highly compact SOI third-order microring add-drop filters were fabricated and their performance agrees well simulation. The microrings have a radius of only 2.5 μm, and a filter occupies a very small footprint of only ~ 5×15 μm^2, which is believed to be the smallest one ever reported in third-order microring add-drop filters. The demonstrated filter has a very large free spectral range of 32 nm around 1.55 μm. The add-drop crosstalk is ~ -20 dB, which should be further reduced for practical applications of add-drop multiplexing. Ideally, without resonance wavelength mismatch, the theoretical add-drop crosstalk can be reduced to ~ -30 dB. Box-like channel dropping responses were achieved with an out-of-band signal rejection is ~ 40 dB. Both simulation and experiments show a very flat passband of ~1nm (125GHz) at 1.55 μm. Within the passband, the simulated group delay is minimum at the center resonance wavelength, and the delay slope is between -2 ps/nm and 2 ps/nm, indicating a small chromatic dispersion. For WDM applications, with the demonstrated channel dropping response, it is feasible to implement around 20 200GHz-spaced dropping channels with adjacent channel cross-talk of -30 dB. The corresponding spectral efficiency can be up to ~ 0.7 bit/s/Hz for the well-known non-return-to-zero (NRZ) format, which is estimated with the ratio between the -3dB passband and the channel spacing.

Acknowledgments

This work was supported in part by a grant from the Defense Threat Reduction Agency (DTRA) under contract HDTRA1-07-C-0042, and in part by the National Science Foundation (NSF) under contract ECCS-0701448.

#86165 - $15.00 USD Received 9 Aug 2007; revised 5 Oct 2007; accepted 9 Oct 2007; published 24 Oct 2007